Imaging Features of Benign and Malignant Ampullary and Periampullary Lesions[1]

Paul Nikolaidis, MD
Nancy A. Hammond, MD
Kevin Day, MD
Vahid Yaghmai, MD
Cecil G. Wood III, MD
David S. Mosbach, MD
Carla B. Harmath, MD
Myles T. Taffel, MD
Jeanne M. Horowitz, MD
Senta M. Berggruen, MD
Frank H. Miller, MD

The ampulla of Vater is an important anatomic landmark where the common bile duct and main pancreatic duct converge in the major duodenal papilla. Imaging evaluation of the ampulla and periampullary region poses a unique diagnostic challenge to radiologists because of the region's complex and variable anatomy and the variety of lesions that can occur. Lesions intrinsic to the ampulla and involved segment of the biliary tree can be neoplastic, inflammatory, or congenital. Neoplastic lesions include ampullary adenocarcinomas and adenomas, which often are difficult to differentiate, as well as pancreatic or duodenal adenocarcinomas, pancreatic neuroendocrine tumors, and cholangiocarcinomas. Ultrasonography (US), computed tomography, magnetic resonance (MR) imaging, and MR cholangiopancreatography are commonly used to evaluate this region. Endoscopic retrograde cholangiopancreatography or endoscopic US examination may be necessary for more definitive evaluation. Periampullary conditions in the duodenum that may secondarily involve the ampulla include neoplasms, duodenitis, duodenal diverticula, and Brunner's gland hyperplasia or hamartomas. Because these lesions can exhibit a wide overlap of imaging features and subtle or nonspecific imaging findings, diagnosis is made on the basis of patient age, clinical history, and imaging and laboratory findings. Given the complexity of imaging evaluation of the ampulla and periampullary region, it is essential for radiologists to understand the variety of lesions that can occur and recognize their imaging characteristics.

Abbreviations: CBD = common bile duct, ERCP = endoscopic retrograde cholangiopancreatography, GIST = gastrointestinal stromal tumor, GRE = gradient echo, HASTE = half-Fourier acquisition single-shot turbo spin-echo, IPMN = intraductal papillary mucinous neoplasm, MRCP = MR cholangiopancreatography, PNET = pancreatic neuroendocrine tumor

RadioGraphics 2014; 34:624–641

Published online 10.1148/rg.343125191

Content Codes: CT GI MR OI

[1]From the Department of Radiology, Northwestern Memorial Hospital and Northwestern University Feinberg School of Medicine, 676 N Saint Clair St, Suite 800, Chicago, IL 60611 (P.N., N.A.H., K.D., V.Y., C.G.W., D.S.M., C.B.H., J.M.H., S.M.B., F.H.M.); and Department of Radiology, George Washington University School of Medicine and Health Sciences, Washington, DC (M.T.T.). Presented as an education exhibit at the 2011 RSNA Annual Meeting. Received September 4, 2012; revision requested November 14; final revision received October 29, 2013; accepted October 31. For this journal-based SA-CME activity, the authors, editor, and reviewers have no financial relationships to disclose. **Address correspondence to** P.N. (e-mail: *p-nikolaidis@northwestern.edu*).

SA-CME LEARNING OBJECTIVES

After completing this journal-based SA-CME activity, participants will be able to:

- Describe the anatomy of the ampulla and periampullary region.
- Discuss the primary imaging modalities used for evaluation of the ampulla and periampullary region.
- Describe the imaging features of various ampullary and periampullary lesions.

See www.rsna.org/education/search/RG.

TEACHING POINTS

See last page

Introduction

The ampulla of Vater is located in the major duodenal papilla and represents the junction of the common bile duct (CBD) and main pancreatic duct of Wirsung (Fig 1). The term *ampulla* is defined as a dilated common channel that is formed where the two ducts combine. However, the use of this terminology is controversial because the presence of a common channel is inconstant, and actual dilatation of the common channel is unusual.

Teaching Point

The joining of the CBD and main pancreatic duct may occur in three ways. Most commonly (60%), the CBD and main pancreatic duct join to form a common channel that is 1–8 mm in length. Less often (38%), a common channel is not present, and instead there is a single orifice in the papilla that contains a separate opening for each duct (double-barrel configuration). Rarely (2%), there are two separate orifices in the papilla that drain the CBD and main pancreatic duct separately (1).

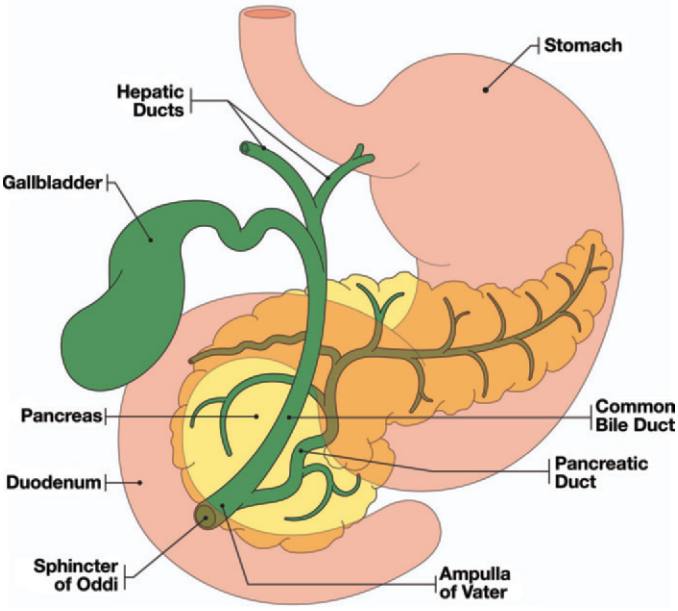

Figure 1. Drawing shows the ampulla and periampullary region, which includes the duodenum, pancreas, and CBD.

Teaching Point

The ampulla of Vater is surrounded by the sphincter of Oddi, a 1-cm structure composed of smooth muscle that regulates the flow of bile and pancreatic juices into the duodenum. The sphincter of Oddi surrounds a portion of the distal CBD, the distal main pancreatic duct, and the common channel (or, depending on the anatomy, the distal parallel channels). The smooth muscle is interspersed with glandular tissue that drains into the ampulla of Vater (1).

The major duodenal papilla is located along the second or third portion of the duodenum (2). At cross-sectional imaging, the major duodenal papilla normally is 1 cm or less in diameter. On contrast material–enhanced images, its enhancement is similar to that of the adjacent duodenal mucosa (2,3).

Given the importance of these anatomic structures, it is essential for radiologists to understand the variety of lesions that can occur in the ampulla and periampullary region (Table).

Ampullary and Periampullary Neoplasms

Ampullary Cancer

Teaching Point

Ampullary cancer (adenocarcinoma) is a rare malignancy that arises from the distal biliary epithelium of the ampulla of Vater. Because of the central location of the lesion, patients often present with obstructive symptoms early in the disease process. Therefore, tumors may be discovered while they are still small and may be surgically resectable. Ampullary cancer is a rare malignancy, with an age-adjusted incidence of 0.70 per 100,000 men and 0.45 per 100,000 women (4).

Approximately 62% of lesions manifest at imaging as a discrete nodular mass that produces an irregular filling defect at the distal margin of the pancreaticobiliary junction (2). However, in some cases, a discrete tumor in the ampullary area may not be visible at imaging (5). At non–contrast-enhanced CT, the tumor typically appears as a hypoattenuating mass with an attenuation of approximately 40 HU. The tumor usually demonstrates enhancement on arterial and portal venous phase images (6). Its borders may be lobulated or infiltrating (Fig 2). At MR imaging, a visible ampullary tumor will enhance after gadolinium-based contrast agent administration (7). The addition of diffusion-weighted imaging sequences to conventional MR imaging has more recently been shown to improve detection of ampullary carcinoma (5). At MRCP, ampullary tumors typically manifest as a filling defect or focal stricture at the distal end of a dilated CBD (7). Dilatation of both the biliary and pancreatic ducts is seen in approximately 52% of cases (2). If the mass does not fully obstruct the biliary and pancreatic ducts after their junction, or when there are separate duodenal openings for the biliary and pancreatic ducts, the double-duct sign may be absent (2). In cases where duct dilatation is seen at imaging without a visible mass, the tumor may not be evident even at endoscopy, and diagnosis may require papillotomy and deep biopsy.

Ampullary Adenoma

Ampullary adenomas are uncommon premalignant lesions that may undergo malignant transformation into adenocarcinoma. They may occur spontaneously or in the context of familial

Symptoms, Imaging Findings, and Diagnosis of Ampullary and Periampullary Lesions

Lesion	Clinical History and Symptoms	Imaging Findings	Diagnostic Methods
Ampullary cancer	Painless jaundice, pruritus, abdominal pain, weight loss, fever	Irregular nodular mass at the distal margin of the pancreaticobiliary junction; less commonly, the tumor is visible only at endoscopy	CT, MR imaging, endoscopy, histopathology
Ampullary adenoma	Painless jaundice, pruritus, abdominal pain, weight loss, fever	Ampullary soft-tissue mass (>1 cm), irregular ampullary margin, extrahepatic biliary dilatation, pancreatic duct dilatation	CT, MR imaging, endoscopy, histopathology
Distal CBD (extrahepatic) cholangiocarcinoma	Painless jaundice, pruritus, abdominal pain, weight loss, fever	Biliary dilatation with abrupt termination at the level of the mass, duct-wall thickening, intraductal polypoid mass, delayed enhancement	CT, MR imaging, endoscopy, histopathology
Duodenal adenocarcinoma	Patients typically aged 50–70 years, with nonspecific symptoms (abdominal pain, nausea, vomiting)	Polypoid or intraluminal mass with eccentric wall thickening; relatively hypovascular	CT, MR imaging, endoscopy, histopathology
GIST	Asymptomatic or nonspecific symptoms (early satiety, bloating)	Variable appearance, from small homogeneous mass to large necrotic mass; endophytic or exophytic to the bowel lumen	CT, MR imaging, endoscopy, histopathology
Periampullary lipoma	Asymptomatic	Smooth well-marginated mass with fat attenuation at CT and fat signal intensity at MR	CT or MR imaging
Pancreatic adenocarcinoma	Painless jaundice, pruritus, abdominal pain, weight loss, fever	Heterogeneously enhancing lesion that is hypovascular relative to the normal pancreas, with progressive delayed enhancement; dilated pancreatic duct and CBD (if periampullary)	CT, MR imaging, endoscopy, histopathology
PNET	Variable, depending on type of tumor, but typically without obstructive symptoms	CT: Homogeneously enhancing lesion in arterial phase MR imaging: T1 signal hypointensity and T2 signal hyperintensity, with enhancement characteristics similar to those at CT; lesions may be cystic	CT, MR imaging, endoscopy, histopathology; hormone levels for functional tumors
IPMN (main duct type)	Asymptomatic or pancreatitis-like symptoms	Dilated main pancreatic duct with bulging of the papilla into duodenal lumen; filling defects within the duct may be enhancing (mural nodules) or nonenhancing (mucin)	CT, MR imaging, endoscopy, histopathology
Other cystic pancreatic neoplasms	Variable	Variable	CT, MR imaging, endoscopic US, histopathology
Papillary stenosis (benign)	Pancreatitis, jaundice, pain	MRCP and ERCP: CBD dilatation with normal (< 12.3-mm) papilla	MRCP, ERCP

Note.—CT = computed tomography, ERCP = endoscopic retrograde cholangiopancreatography, GIST = gastrointestinal stromal tumor, IPMN = intraductal papillary mucinous neoplasm, MR = magnetic resonance, MRCP = MR cholangiopancreatography, PNET = pancreatic neuroendocrine tumor, US = ultrasonography.

(continues)

Symptoms, Imaging Findings, and Diagnosis of Ampullary and Periampullary Lesions *(continued)*

Lesion	Clinical History and Symptoms	Imaging Findings	Diagnostic Methods
Choledocholithiasis	Right upper-quadrant pain, nausea, vomiting, abnormal liver function test results	CT: visible hyperattenuating stones surrounded by low-attenuation bile or soft tissue MR imaging: CBD filling defect and obstruction, smooth symmetric papillary edema, increased papillary enhancement	US, CT (less sensitive), MRCP, ERCP
Pancreatic divisum	Typically asymptomatic	Noncommunicating dorsal duct draining into minor papilla independent of the CBD	CT, MRCP, or ERCP
Santorinicele	Pancreatitis	MRCP: cystic dilatation of the accessory pancreatic duct, with sparing of the minor papilla	MRCP, preferably with secretin administration
Choledochocele (type III choledochal cyst)	Typically manifests in childhood with classic triad of abdominal pain, palpable mass, and jaundice	MRCP: cystic mass contiguous with the distal CBD	MRCP or ERCP
Groove pancreatitis	Chronic pancreatitis	Sheetlike mass in pancreaticoduodenal groove area near the minor papilla with delayed enhancement; thickening and cystic changes in duodenal wall	CT, MR imaging, histopathology
Autoimmune pancreatitis and IgG4-related sclerosing cholangitis	Abdominal pain, jaundice, chronic pancreatitis	Focal or diffuse enlarged sausage-shaped pancreas with surrounding capsule-like rim; evidence of sclerosing cholangitis or pseudotumorous lesions	Radiologic and histologic features, serum IgG4 levels
Pancreaticoduodenal artery pseudoaneurysm	History of pancreatitis	Rounded mass in pancreaticoduodenal groove; enhancement pattern follows blood pool, depending on degree of patency of pseudoaneurysm	Color Doppler US; CT or MR angiography
Brunner's gland hyperplasia and hamartoma	Usually asymptomatic; may manifest with obstruction of the duodenum, CBD, or pancreatic duct	Hyperplasia: typically multiple nodular filling defects (< 5 mm) in proximal duodenum Hamartoma: typically larger solitary mass	CT, MR imaging, fluoroscopy, endoscopy, histopathology
Duodenitis	Abdominal pain	CT or MR imaging: thickened duodenal wall with variable enhancement	CT, MR imaging, endoscopy
Duodenal Crohn disease	Fatigue, diarrhea with abdominal pain, weight loss, possible bleeding	Thickened duodenal folds, ulcers, strictures, fistula formation	CT, MR imaging, fluoroscopy, endoscopy, histopathology
Duodenal diverticula	Usually asymptomatic unless inflamed (duodenal diverticulitis)	Round periduodenal structure containing air, fluid, or debris; fat stranding; wall thickening (if diverticulitis)	CT, MR imaging
Duodenal perforation and transection	Abdominal pain, but physical examination may not be impressive because of retroperitoneal location	Periduodenal fluid, wall thickening or edema, fat stranding, possible extraluminal air	CT, fluoroscopy, exploratory laparotomy

Note.—CT = computed tomography, ERCP = endoscopic retrograde cholangiopancreatography, GIST = gastrointestinal stromal tumor, IPMN = intraductal papillary mucinous neoplasm, MR = magnetic resonance, MRCP = MR cholangiopancreatography, PNET = pancreatic neuroendocrine tumor, US = ultrasonography.

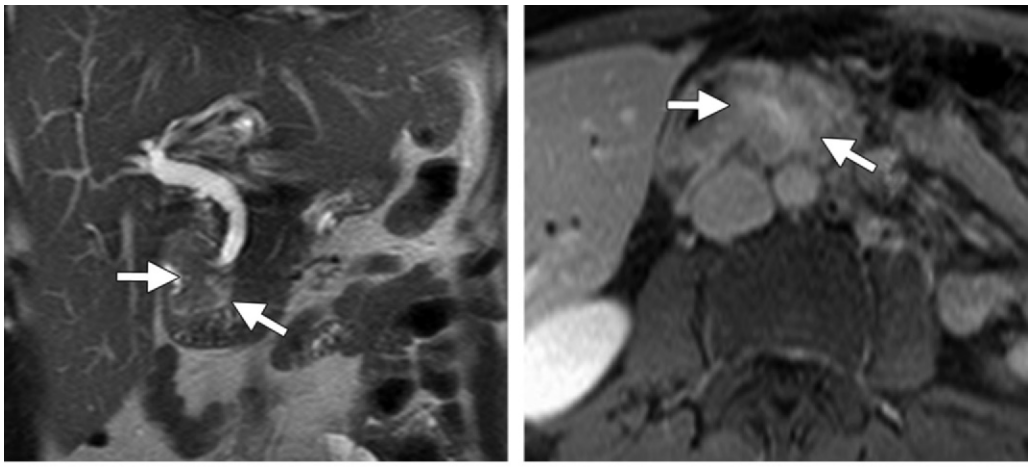

a. b.

Figure 2. Ampullary adenocarcinoma in a 71-year-old man. **(a)** Coronal T2-weighted half-Fourier acquisition single-shot turbo spin-echo (HASTE) (Siemens Healthcare, Erlangen, Germany) MR image shows a mildly hyperintense lobulated mass (arrows) arising from the ampulla, with associated dilatation of the CBD. **(b)** Axial contrast-enhanced fat-saturated T1-weighted gradient-echo (GRE) MR image shows the infiltrative nature of the heterogeneously enhancing ampullary mass (arrows).

a. b.

Figure 3. Ampullary adenoma in a 65-year-old man. **(a)** Coronal T2-weighted HASTE MR image shows a lobulated mass in the region of the ampulla (arrow), with mild dilatation of the CBD and pancreatic duct. **(b)** Image from endoscopic US shows a filling defect (arrow) caused by the echogenic lobulated mass, which arises from the region of the ampulla and fills the distal CBD.

polyposis syndrome (8). The prevalence of ampullary adenomas has been estimated as 0.04%–0.12% in autopsy series (9). Cross-sectional imaging findings of ampullary adenomas (Fig 3) have not been described extensively. In one study, common CT findings of an ampullary adenoma included an ampullary soft-tissue mass greater than 1 cm, an irregular margin of the ampulla, extrahepatic biliary duct dilatation, and pancreatic duct dilatation (10). At imaging, the tumors are more readily visualized when the duodenum is well distended.

Distal CBD (Extrahepatic) Cholangiocarcinoma

A cholangiocarcinoma is an adenocarcinoma that arises from the epithelial cells of the biliary duct. The reported age-adjusted incidence of extrahepatic cholangiocarcinoma is 1.2 per 100,000 men and 0.8 per 100,000 women (11). There are two gross subtypes of extrahepatic cholangiocarcinoma: infiltrating and polypoid. A common imaging feature of both subtypes is biliary duct dilatation, which terminates abruptly at the level of the mass (12). At cross-sectional

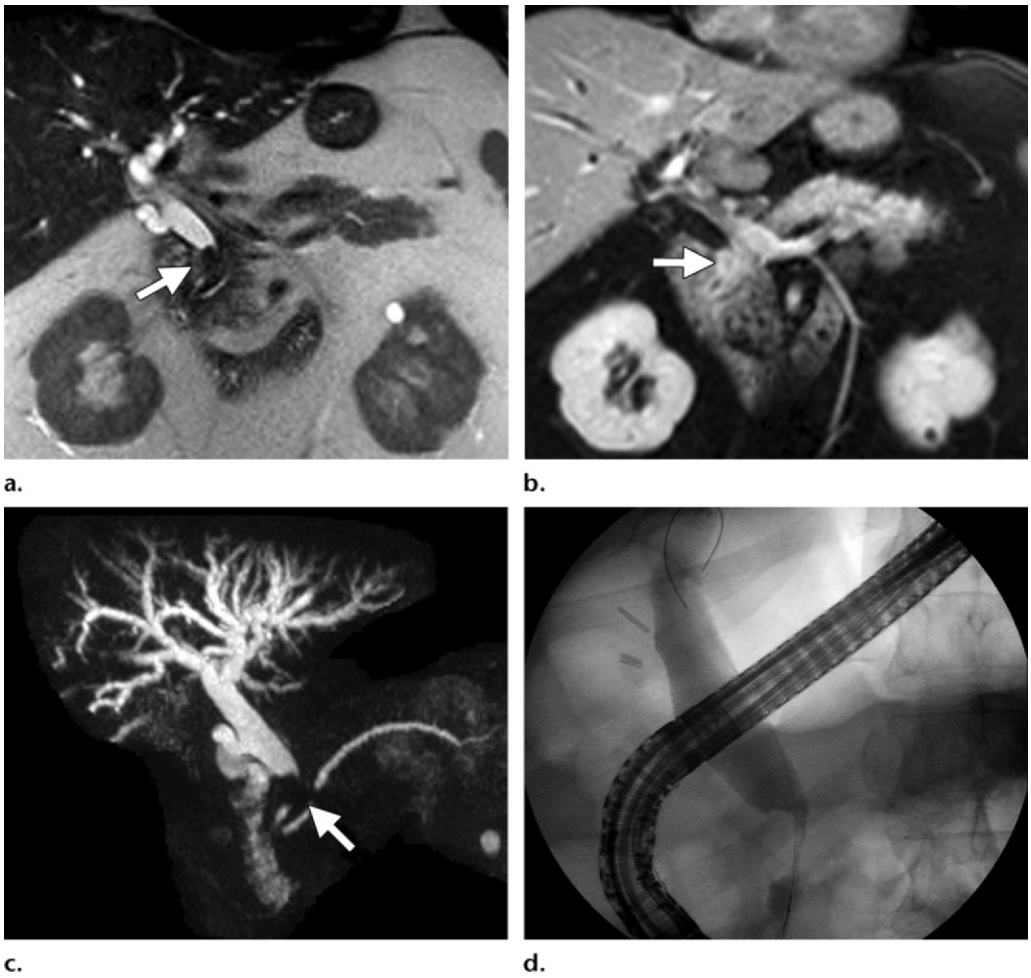

Figure 4. Distal cholangiocarcinoma in a 59-year-old woman. **(a)** Coronal T2-weighted HASTE MR image shows dilatation of the CBD to the level of a hypointense filling defect (arrow). There is significant intra- and extrahepatic bile duct dilatation to the level of the mass, and the CBD below the mass is normal in caliber. **(b)** Coronal contrast-enhanced fat-saturated T1-weighted GRE MR image shows enhancement of the filling defect in the distal CBD (arrow), a finding that confirms a soft-tissue mass rather than a stone in the CBD. **(c)** Coronal MRCP image shows the filling defect in the distal CBD (arrow) and dilatation of the biliary tree. **(d)** ERCP image shows an eccentric and irregular filling defect in the CBD, which corresponds to the mass seen at MR imaging.

imaging, an infiltrating cholangiocarcinoma is typically characterized by ductal wall thickening and sudden luminal obliteration (2). A polypoid lesion may manifest at imaging as an intraductal polypoid mass that typically does not cause complete obstruction (Fig 4) (2). A cholangiocarcinoma typically is hypointense relative to the liver parenchyma on T1-weighted MR images and hyperintense on T2-weighted MR images (13). It may also demonstrate homogeneous slow enhancement and typically is more conspicuous on fat-suppressed MR images (13).

Duodenal Adenocarcinoma

A periampullary duodenal adenocarcinoma is a rare tumor that typically abuts but spares or only partially involves the major duodenal papilla (7). At imaging, the tumor manifests as either a polypoid or intraluminal mass, with eccentric duodenal wall thickening (14,15). Between 1985 and 2005, 67,843 patients in the United States were diagnosed with small-bowel malignancies, with adenocarcinoma accounting for 37% of these cases (16). However, the true incidence of periampullary duodenal adenocarcinoma is not known. Duodenal adenocarcinoma more commonly involves a relatively short segment of the bowel and results in gradual luminal narrowing (17). If there is ampullary involvement, biliary dilatation may be seen at imaging. Larger lesions may cause luminal obstruction and gastric distention. At multiphasic CT studies, periampullary duodenal adenocarcinoma is typically hypovascular (Fig 5) (17). At MR imaging, the lesions manifest as polypoid fungating masses or areas of eccentric wall thickening (2).

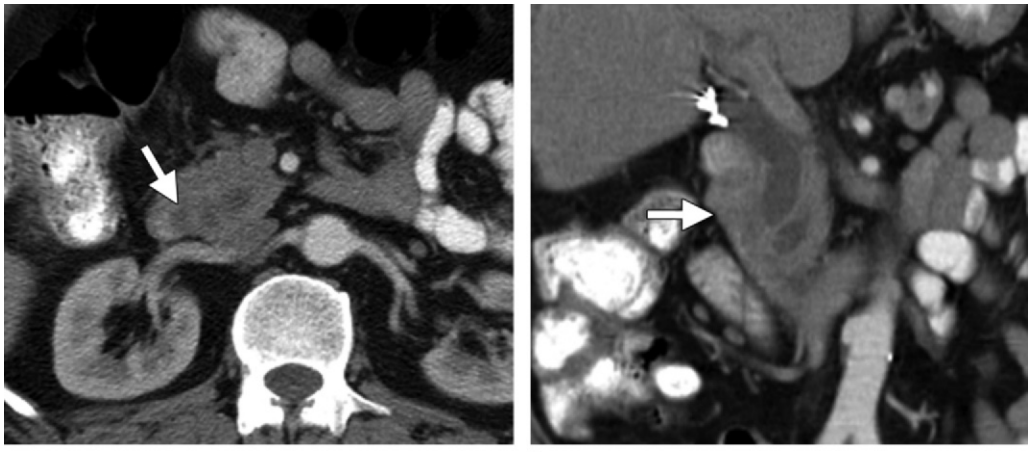

a. b.

Figure 5. Duodenal adenocarcinoma in a 69-year-old man. **(a)** Axial contrast-enhanced CT image obtained in the arterial phase shows a hypoattenuating mass in the medial wall of the second portion of the duodenum (arrow). **(b)** Coronal contrast-enhanced reformatted CT image obtained in the arterial phase shows the duodenal mass (arrow), with dilatation of the CBD and pancreatic duct caused by obstruction of the ampulla.

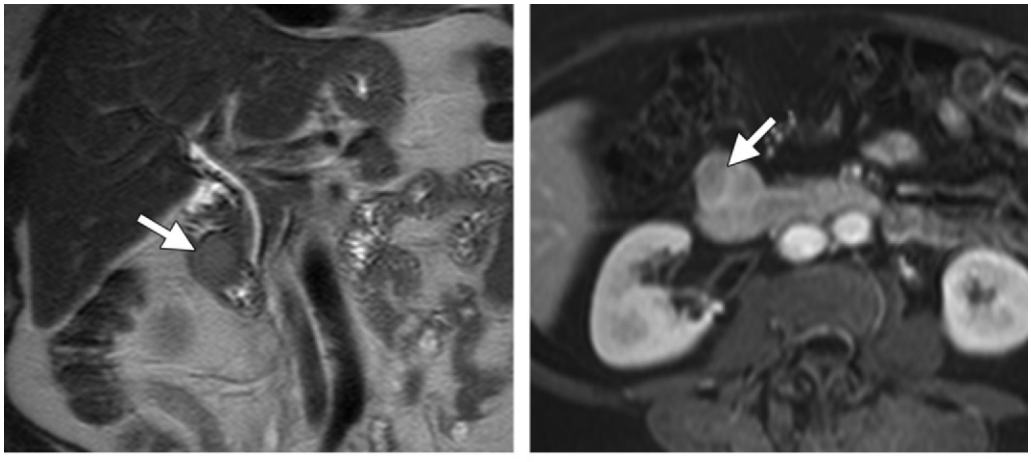

a. b.

Figure 6. Duodenal GIST in a 61-year-old man. **(a)** Coronal T2-weighted HASTE MR image shows a well-circumscribed mass that extends into the duodenal lumen at the level of the ampulla (arrow). The hyperintensity of the mass is a finding indicative of a GIST. No associated dilatation of the biliary or pancreatic duct is seen. **(b)** Axial contrast-enhanced fat-saturated T1-weighted GRE MR image shows the round mildly enhancing duodenal mass (arrow).

Gastrointestinal Stromal Tumor

GISTs are tumors of mesenchymal origin. The age-adjusted yearly incidence of GIST is 0.68 per 100,000 persons (18). Periampullary stromal tumors account for approximately 3%–5% of all GISTs (19). The small intestine is the second most common site of involvement, after the stomach (18). The masses may be intramural or intraluminal (20). The imaging appearance of GISTs can vary from small homogeneous masses to large necrotic masses (21). Tumors may be endophytic or exophytic to the bowel (21). Smaller tumors typically manifest at imaging as sharply demarcated, smooth-walled, homogeneous soft-tissue masses with at least moderate contrast enhancement (Fig 6). They typically show low signal intensity on T1-weighted MR images and intermediate to high signal intensity on T2-weighted MR images (20). Larger tumors tend to undergo central necrosis and cavitation and demonstrate heterogeneous enhancement at imaging.

Periampullary Lipoma

A periampullary duodenal lipoma is a benign lesion that is frequently asymptomatic and typically occurs in men aged 70-80 years (14). Small-bowel lipomas are relatively rare, with few cases described in the literature (22). The prevalence of

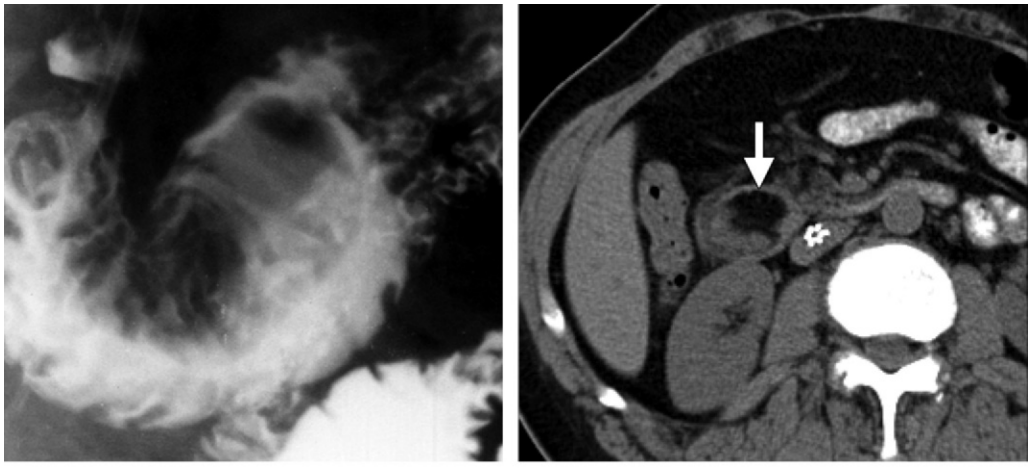

a. b.

Figure 7. Periampullary duodenal lipoma in a 70-year-old man. **(a)** Spot image from a biphasic upper gastrointestinal study shows a smoothly marginated filling defect that extends from the second to third portion of the duodenum. This finding was slightly mobile at fluoroscopy. **(b)** Axial nonenhanced CT image shows an intraluminal mass with attenuation of fat in the second portion of the duodenum (arrow), a finding consistent with a lipoma.

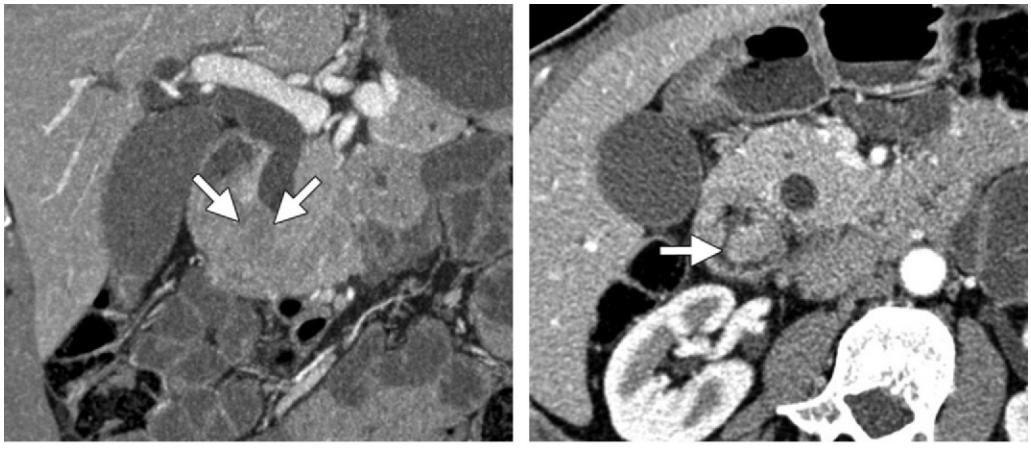

a. b.

Figure 8. Pancreatic adenocarcinoma in a 68-year-old man who presented with painless jaundice. **(a)** Coronal contrast-enhanced reformatted CT image obtained in the portal venous phase demonstrates a hypoattenuating mass in the pancreatic head that involves the ampullary region (arrows). There is abrupt termination of the dilated CBD because of the mass. **(b)** Axial contrast-enhanced CT image obtained in the pancreatic phase demonstrates tumor extension through the ampulla and papilla into the duodenal lumen (arrow).

periampullary lipomas is unknown. At imaging, they appear as smooth well-marginated masses. At CT, they demonstrate fat attenuation (<–20 HU) (Fig 7) (22). At MR imaging, they show fat signal intensity with all sequences.

Pancreatic Adenocarcinoma

Pancreatic adenocarcinoma may occur near the ampulla of Vater and manifests as an ampullary or more likely periampullary mass. Depending on the location of the tumor and its relationship to the pancreaticobiliary tree, patients may present with obstructive symptoms. Approximately 43,920 patients are diagnosed with pancreatic cancer in the United States each year (23). Most of these cancers (85%) are ductal adenocarcinomas. At contrast-enhanced CT and MR imaging, a pancreatic adenocarcinoma typically manifests as a heterogeneously enhancing lesion that is hypovascular relative to the normal pancreatic parenchyma (Fig 8) (17). A pancreatic adenocarcinoma is hypointense relative to the normal pancreas on fat-suppressed T1-weighted MR images, shows decreased enhancement relative to the pancreas on arterial phase MR images, and progressively enhances on more

delayed phase MR images (24). On T2-weighted MR images, the tumor usually is minimally hypointense relative to the pancreas and therefore difficult to visualize (25).

Pancreatic Neuroendocrine Tumor

PNETs constitute a rare subtype of tumors that arise from the endocrine cells in or near the pancreas (26). A conservative estimate of the incidence of PNETs in the United States is approximately 25–30 per 100,000 individuals (27). The most common location for these tumors is the gastrinoma triangle, which is defined by the junction of the cystic and common hepatic ducts, the junction of the second and third portions of the duodenum, and the border of the body and tail of the pancreas (26). PNETs are unlikely to cause ampullary or ductal obstruction. They are hypoattenuating on nonenhanced CT images (28). At MR imaging, they typically are hypointense on fat-suppressed T1-weighted images and hyperintense on T2-weighted images (12,29). At contrast-enhanced CT or MR imaging, PNETs demonstrate homogeneous hyperenhancement relative to the normal pancreatic parenchyma during the arterial and capillary phases (Fig 9) (12,30).

In a recent series of 78 cases of PNET, it was reported that 18% of PNETs are partially or completely cystic. More typically, cystic PNETs demonstrate peripheral contrast enhancement; however, some can appear entirely cystic at imaging. Although cystic PNETs have traditionally been believed to represent larger tumors with cystic degeneration, a more recent series showed that the incidence of small and larger cystic PNETs is similar (31).

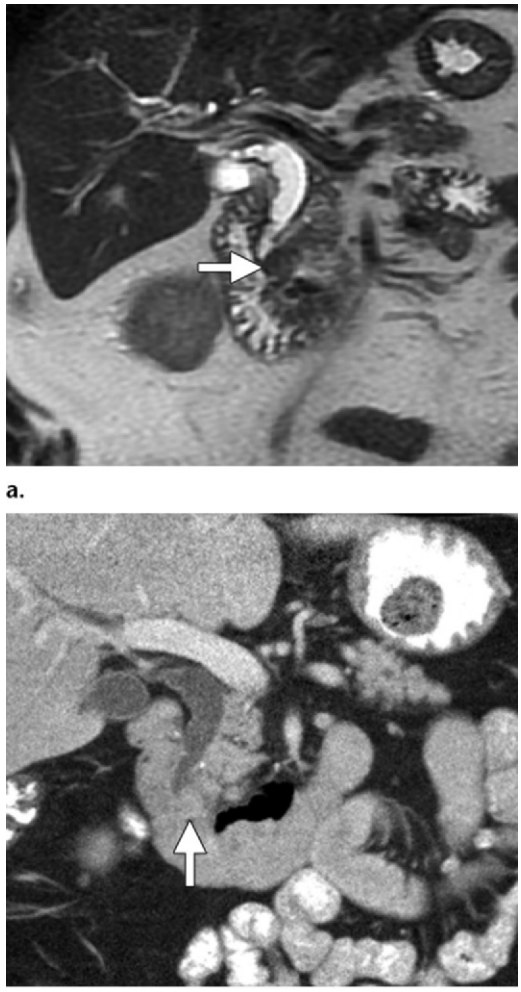

Figure 9. PNET in a 42-year-old woman. **(a)** Coronal T2-weighted HASTE MR image shows a round mass (arrow) in the pancreatic head adjacent to the ampulla, with dilatation of the CBD. **(b)** Coronal contrast-enhanced reformatted CT image obtained in the portal venous phase shows an enhancing mass (arrow) that corresponds to the lesion in **a**, with dilatation of the CBD and mild dilatation of the intrahepatic biliary duct.

Intraductal Papillary Mucinous Neoplasm (Main Duct Type)

IPMNs are a group of neoplasms in the biliary duct or pancreatic duct that cause cystic dilatation from excessive mucin production and accumulation. The true incidence of IPMNs is unknown because many are small and asymptomatic. However, in a series of 2832 consecutive CT scans of adults with no history of pancreatic lesions, 73 cases of pancreatic cysts (2.6%) were identified (32). Many of these cases likely were IPMNs, given that IPMNs account for 20%–50% of cystic pancreatic neoplasms. There are three main types of pancreatic IPMNs: main duct, branch duct, and combined. A main duct IPMN commonly causes dilatation of the papilla, with bulging of the papilla into the duodenal lumen (33). Filling defects caused by mural nodules or mucin may be seen at MRCP or ERCP. At CT and MR imaging, filling defects caused by mural nodules enhance, while filling defects caused by mucin do not enhance (33).

Other Cystic Pancreatic Neoplasms

In addition to IPMNs, the most common cystic pancreatic lesions are pancreatic pseudocysts, serous cystic neoplasms, solid pseudopapillary neoplasms, and mucinous cystic neoplasms. A combination of factors that include patient age, clinical history, and imaging and laboratory findings is often required for diagnosis. With the exception of serous cystic neoplasms, cystic pancreatic lesions that occur in the periampullary region could cause ductal obstruction.

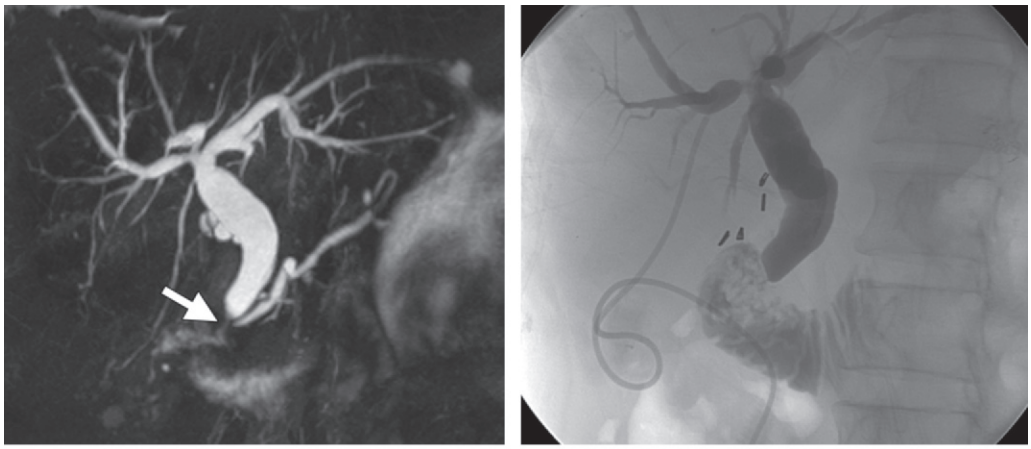

a. b.

Figure 10. Papillary stenosis in a 45-year-old woman who underwent cholecystectomy 12 years earlier. US examination (not shown) showed increased dilatation of the CBD. **(a)** Maximum intensity projection image from navigator-triggered MRCP shows dilatation of the CBD to the level of a tight stricture that involves the ampulla (arrow). No filling defects are seen that would suggest a stone. No abnormal enhancement was seen on corresponding MR images (not shown) that would suggest an ampullary mass. **(b)** ERCP image shows dilatation of the CBD and intrahepatic biliary tree. Brushings were negative for malignancy, and endoscopic US showed no focal abnormality.

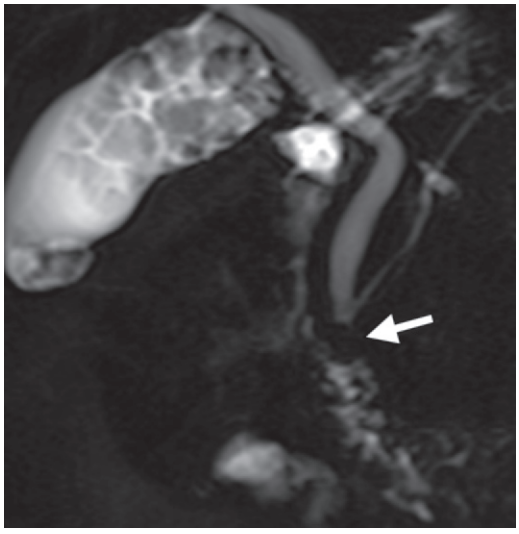

Figure 11. Choledocholithiasis in a 39-year-old woman. Coronal rapid acquisition with relaxation enhancement (RARE) MRCP image shows a dilated CBD with a filling defect in the ampullary region (arrow), a finding consistent with a stone in the CBD. The CBD is mildly dilated, but the pancreatic duct is not. Numerous additional stones are seen in the gallbladder. The findings were confirmed at endoscopy.

Non-neoplastic Lesions

Intrinsic Bile Duct Processes

Teaching Point

Papillary Stenosis.—Papillary stenosis is the blockage of bile or pancreatic fluid flow at the sphincter of Oddi in the absence of a mass or inflammatory lesion at the ampulla. It may manifest with pancreatitis, jaundice, or pain. The most common cause of papillary stenosis is sphincter of Oddi dysfunction, which can be either structural or functional. In the general population, the prevalence of sphincter of Oddi dysfunction is 1.5% (34). At imaging, benign and malignant causes of papillary stenosis are difficult to differentiate. In a recent CT study, a papillary size of less than 12.3 mm was found to be the only independently reliable variable for differentiating benign from malignant causes of papillary stenosis (6). At MR imaging and MRCP, papillary stenosis appears as dilatation of the bile duct or pancreatic duct, with no definite mass lesion seen (7). ERCP, endoscopic US, or serial follow-up studies may be helpful to determine the cause of papillary stenosis in these patients (Fig 10) (35).

Choledocholithiasis.—Gallstone disease is very common and affects 15% of the population. Of these cases, 10%–15% develop choledocholithiasis (36). CT is not as sensitive as MRCP or ERCP for detection of biliary stones, with a sensitivity of 72%–78% reported in the literature (37). If a ductal stone is visible at CT, it classically appears as a hyperattenuating lesion surrounded by hypoattenuating bile and ampullary soft tissue (17,38). With the exception of stones less than 3 mm in size, MRCP is highly sensitive for choledocholithiasis, with an overall pooled sensitivity of 95% reported in one meta-analysis of patients with suspected biliary disease (Fig 11)

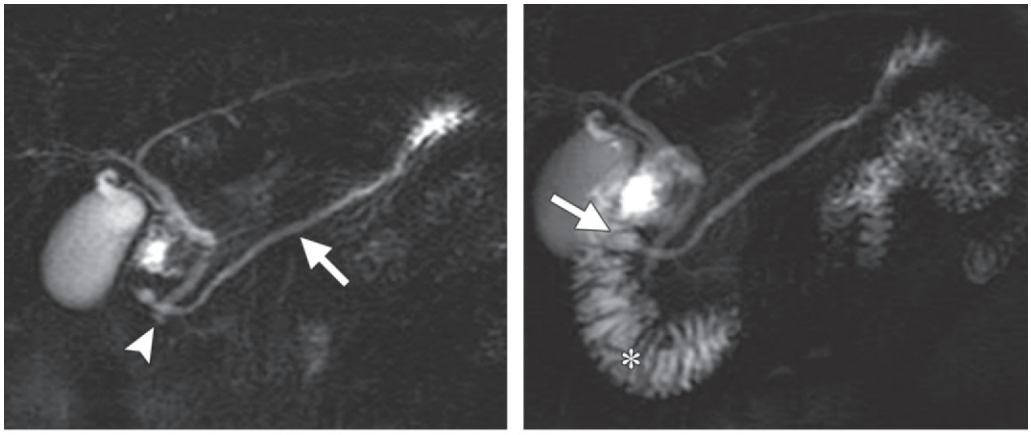

a. b.

Figure 12. Pancreas divisum and santorinicele. **(a)** Coronal MRCP image shows pancreas divisum, with the dorsal duct draining into a minor papilla (arrow) independent of the CBD (arrowhead). The distal dorsal duct is prominent. The ventral duct is not shown. **(b)** Coronal dynamic MRCP image obtained 5 minutes after secretin administration shows enlargement of the dorsal pancreatic duct and a santorinicele (arrow). Increased pancreatic secretions have resulted in increased duodenal filling (*). (Images courtesy of Naoki Takahashi, MD.)

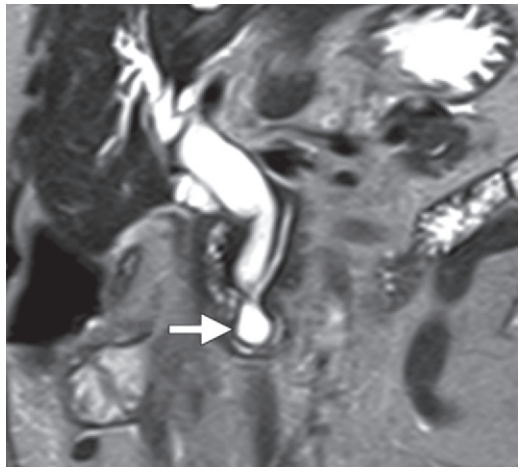

Figure 13. Choledochocele in a 32-year-old man. Coronal T2-weighted HASTE MR image shows a cystic mass at the distal aspect of the CBD that is believed to communicate with the duct (arrow). Extrahepatic biliary dilatation also is seen.

(39). In certain cases, distal choledocholithiasis may cause papillitis and may manifest with MR imaging findings of bile duct obstruction at the papilla, smooth symmetric papillary edema, and increased enhancement of the papilla (7).

Pancreatic Divisum.—Pancreatic divisum is a congenital anomaly of the pancreas due to failure of fusion of the dorsal and ventral pancreatic ducts (15). Pancreatic divisum may be visualized at both CT and MR imaging, where the noncommunicating dorsal duct is seen to drain into the minor papilla independent of the CBD (Fig 12) (40,41). Another well-described imaging finding is the dominant dorsal duct sign, in which a larger dorsal duct is seen relative to a smaller ventral duct (40). Pancreas divisum may be associated with stenosis of the main duct at the minor papilla (40). A relative obstruction to pancreatic exocrine secretory flow through the minor duct and minor papilla may result in pancreatitis in a small number of patients with pancreas divisum (42). In a series of 1825 successful consecutive ERCP procedures, the incidence of pancreas divisum was 7.5% (43).

Santorinicele.—A santorinocele is a cystic dilatation of the accessory pancreatic duct, usually in the setting of pancreatic divisum; however, two case reports have described findings of a santorinicele without pancreatic divisum (44,45). A santorinocele is a rare entity that has primarily been reported in case reports and case series, and the true incidence is unknown. It is most easily diagnosed at MRCP, where it appears as a cystic dilatation with sparing of the minor papilla (Fig 12) (15). Diagnosis at MRCP is aided with administration of intravenous secretin, which improves visualization of the pancreatic ducts (15). Secretin is a hormone secreted by the duodenum in response to increased acid. It causes transient constriction of the sphincter of Oddi and increased production of pancreatic secretions. The effects of intravenous secretin stimulation are greatest 4–10 minutes after injection (46).

Teaching Point

In cases of suspected ampullary stenosis, secretin administration will cause persistent

a.

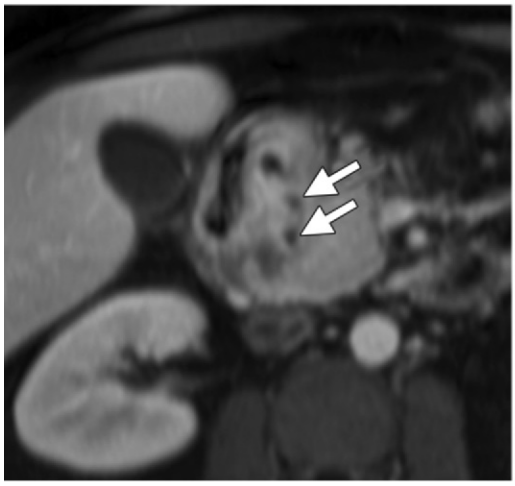

b.

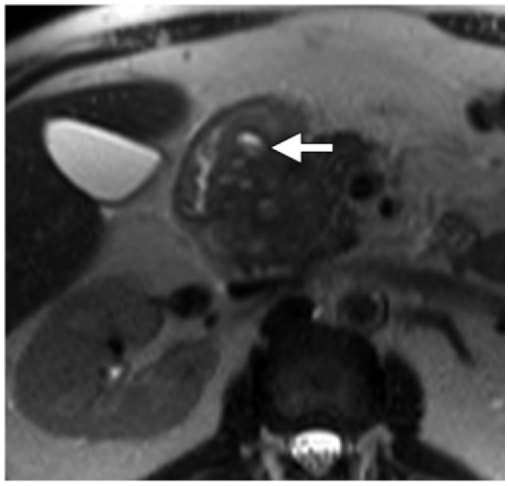

c.

Figure 14. Groove pancreatitis in a 52-year-old man. **(a)** Axial contrast-enhanced CT image obtained in the portal venous phase shows a relatively hypoenhancing mass in the space between the pancreas and duodenum. A few subtle cystic foci are seen in the mass. **(b)** Axial contrast-enhanced fat-saturated delayed phase T1-weighted GRE MR image shows the infiltrative mass occupying the pancreaticoduodenal groove, with delayed enhancement. Distinct areas of low signal intensity, thought to represent cystic dystrophy in the heterotopic pancreatic tissue, are seen (arrows). **(c)** Axial T2-weighted HASTE MR image depicts the small hyperintense cystic foci (arrow). The surrounding low T2 signal intensity indicates underlying fibrosis.

dilatation of the pancreatic duct (46). Increased pancreatic secretions caused by secretin administration will also distend the adjacent duodenum with fluid. On T2-weighted MR images, pancreatic secretions provide a natural contrast with the adjacent ampulla and can improve visualization of ampullary masses (46,47).

Choledochocele.—A choledochocele (type III choledochal cyst) is a cystic dilatation of the intramural portion of the CBD that results in enlargement of the papilla (7,15). Choledochochal cysts are rare in Western countries, with an overall incidence of one per 100,000–150,000 (48). Type III choledochal cysts are the rarest type, accounting for 1%–4% of all cases (48). Their pathogenesis is controversial (7,15). At MRCP, a choledochocele will appear as a cystic mass that is contiguous with the distal bile duct (Fig 13) (49). Diagnosis is important because a choledochocele may cause recurrent bouts of pancreatitis (50).

Periampullary Processes Related to the Pancreas and Duodenum

Groove Pancreatitis.—Groove pancreatitis, a distinct form of chronic pancreatitis, is characterized by inflammation and fibrous tissue formation that affect the pancreaticoduodenal groove between the head of the pancreas, the duodenum, and the CBD. The true prevalence of groove pancreatitis is unknown because only case reports and case series have been published (51). At CT or MR imaging, a sheetlike low-signal-intensity mass with delayed enhancement is seen in the pancreaticoduodenal groove area near the minor papilla (52). Thickening of the duodenal wall and cystic changes along the duodenal wall can also be seen at imaging (Fig 14) (52). A long, smooth, segmental stenosis in the distal or intrapancreatic CBD or a medial shift of the duct may be seen at MRCP. A widening of the space between the distal pancreatic duct and CBD and the duodenal lumen is another characteristic imaging sign (53).

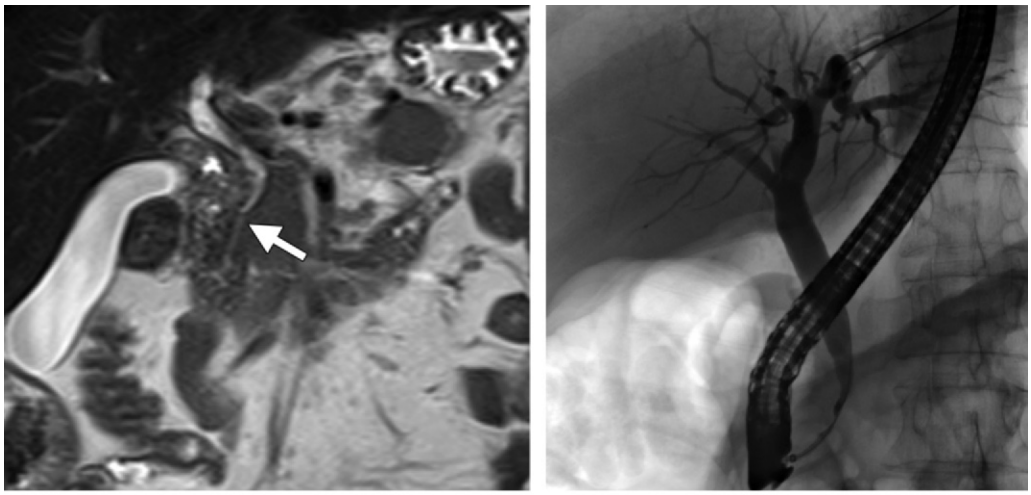

a. b.

Figure 15. Autoimmune pancreatitis with IgG4-related sclerosing cholangitis in a 44-year-old woman. **(a)** Coronal T2-weighted HASTE MR image shows diffuse narrowing of the distal CBD (arrow) and mild upstream dilatation. **(b)** Spot image from ERCP shows mild irregularity in the narrowed distal CBD. The imaging appearance of the CBD normalized after steroid therapy.

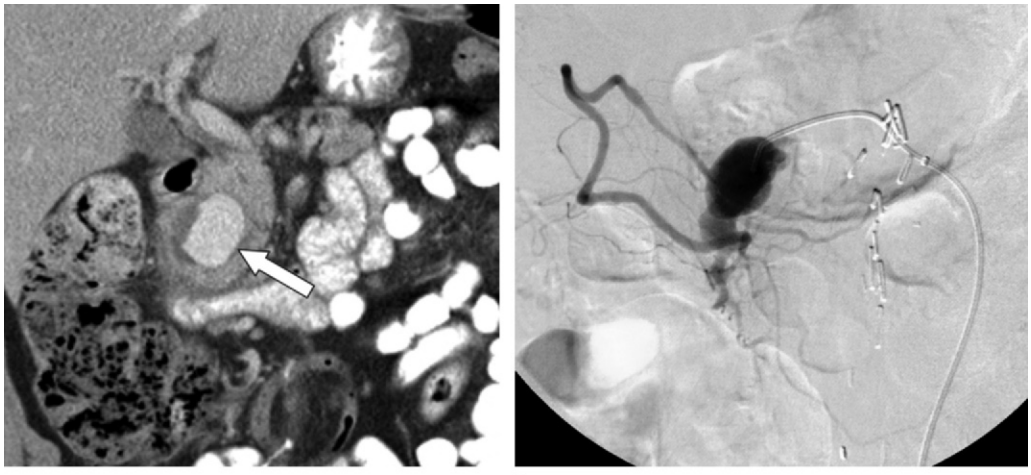

a. b.

Figure 16. Pancreaticoduodenal artery pseudoaneurysm in a 41-year-old man with a history of pancreatitis. **(a)** Coronal contrast-enhanced reformatted CT image obtained in the portal venous phase shows an avidly enhancing mass (arrow) with a rim of peripheral low attenuation in the region of the pancreatic head adjacent to the descending duodenum. **(b)** Spot image from angiography shows a pseudoaneurysm arising from the pancreaticoduodenal artery. The lesion was treated successfully with placement of embolization coils.

Autoimmune Pancreatitis and IgG4-related Sclerosing Cholangitis.—Autoimmune pancreatitis is a benign, IgG4-related, fibroinflammatory form of chronic pancreatitis. Autoimmune pancreatitis is a relatively recently described entity that was first recognized in 1995. Although the true prevalence of this disease is unknown, a recent study that involved 23 institutions in 10 countries registered 1064 patients who met the diagnostic criteria for autoimmune pancreatitis (54). Laboratory studies typically demonstrate elevated serum IgG4 levels, and imaging studies show a focally or diffusely enlarged sausage-shaped pancreas with a capsule-like rim and an irregularly narrowed pancreatic duct (55). The bile ducts, salivary glands, kidneys, and lymph nodes can be involved either synchronously or metachronously (56). At imaging, IgG4 cholangiopathy manifests as sclerosing cholangitis or pseudotumorous lesions (Fig 15) (57). Patients typically respond to steroid therapy.

Pancreaticoduodenal Artery Pseudoaneurysm.—A pancreaticoduodenal artery pseudoaneurysm is a complication associated with acute or chronic pancreatitis and results

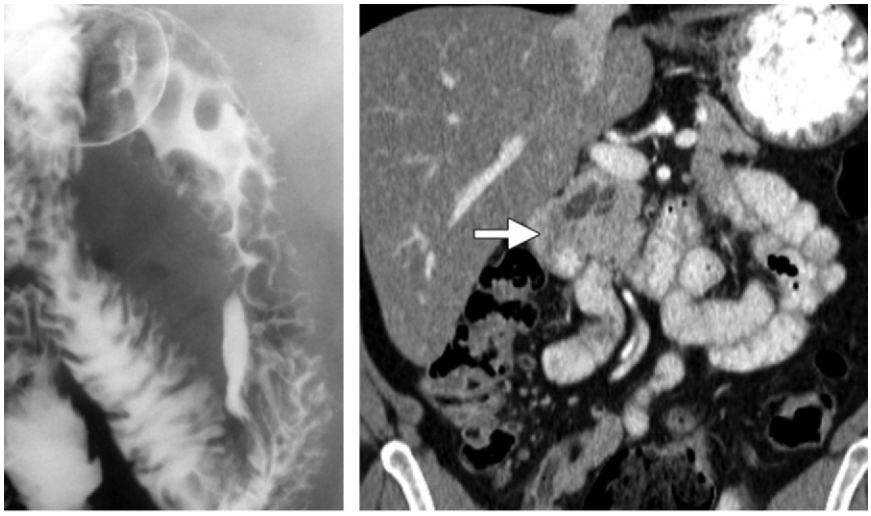

a. b.

Figure 17. Brunner's gland hyperplasia in a 27-year-old woman. **(a)** Spot image from biphasic upper gastrointestinal study shows nodular thickening in the descending portion of the duodenum, a finding consistent with Brunner's gland hyperplasia. **(b)** Coronal contrast-enhanced reformatted CT image obtained in the portal venous phase shows focal thickening of the medial aspect of the duodenum in the region of the ampulla (arrow). Associated dilatation of the CBD and pancreatic duct is seen.

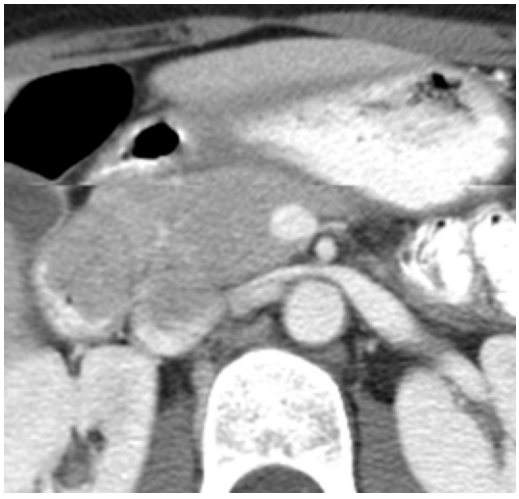

Figure 18. Brunner's gland hamartoma in a 42-year-old man. Axial contrast-enhanced CT image obtained in the portal venous phase shows a homogeneously enhancing nodular mass arising from the second portion of the duodenum. The mass extends exophytically into the lumen of the duodenum, and no dilatation of the stomach, proximal duodenum, or CBD is seen.

from leakage of pancreatic enzymes and erosion of the arterial wall (15). The prevalence of pancreaticoduodenal artery pseudoaneurysms is unknown because only a few case reports have been published (58). At imaging, a round mass that follows the enhancement pattern of blood pool is identified in the pancreaticoduodenal groove. Thin-walled calcifications may be seen at CT, as well as an internal mural thrombus (Fig 16) (15). Although the enhancement pattern follows that of blood pool, the exact imaging features may depend on the degree of patency of the lumen of the pseudoaneurysm. A pseudoaneurysm may rupture into the peritoneum, retroperitoneum, or intestinal lumen (15).

Brunner's Gland Hyperplasia and Hamartoma.—Brunner's glands are submucosal glands located in the proximal two-thirds of the duodenum that produce alkaline secretions to buffer gastric acid (59). Brunner's gland hyperplasia and hamartomas are uncommon benign tumors of the duodenum, with fewer than 200 cases reported (60). There have been reports of Brunner's gland hyperplasia that manifests as acute pancreatitis (60). At imaging, Brunner's gland hyperplasia manifests with solitary or multiple small (<5-mm) nodular filling defects in the proximal duodenum (Fig 17) (61).

The pathogenesis of Brunner's gland hamartoma is unknown. It most commonly occurs along the posterior wall of the first and second portions of the duodenum (61). It is a benign mass that manifests at imaging as a solitary filling defect (59). Patients commonly are asymptomatic but may present with symptoms of duodenal obstruction, intussusception, or CBD or pancreatic duct obstruction (61). On nonenhanced CT images, an isoattenuating mass relative to the adjacent duodenal wall is seen (Fig 18). Peripheral rimlike enhancement or small internal cystic portions may be seen on contrast-enhanced CT images (62).

Duodenitis.—Duodenitis is inflammation of the duodenum in the absence of ulcer formation (14,59). Duodenitis is associated with *Helicobacter pylori* infection, use of nonsteroidal anti-inflammatory drugs, use of ethanol, and gastric acid secretion. Furthermore, inflammation of the duodenal papilla may occur in patients with acquired

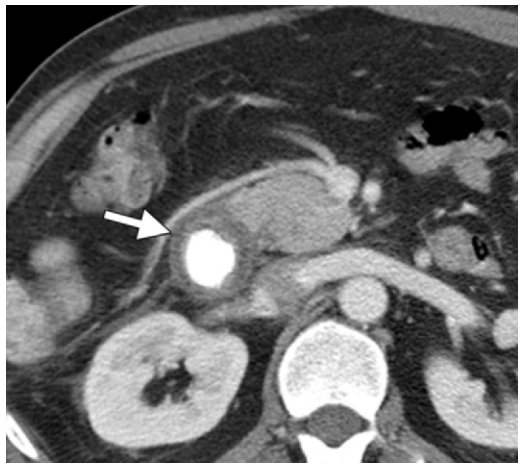

Figure 19. Duodenitis in a 38-year-old woman with epigastric pain and a history of nonsteriodal anti-inflammatory drug use. Axial contrast-enhanced CT image obtained in the portal venous phase shows diffuse thickening of the wall of the descending portion of the duodenum (arrow), a finding that extended into the third portion of the duodenum (not shown).

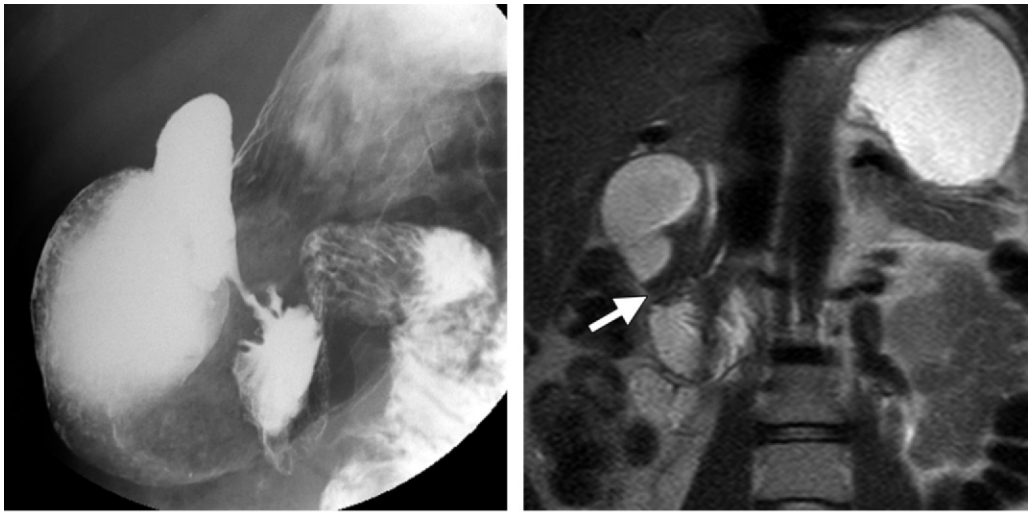

a. b.

Figure 20. Duodenal Crohn disease in a 29-year-old pregnant woman. **(a)** Spot image from a biphasic upper gastrointestional study shows focal narrowing of the second portion of the duodenum, with mild irregularity of the involved mucosa. **(b)** Coronal T2-weighted HASTE MR image shows the narrowed segment at the level of the ampulla (arrow). Dilatation of the stomach and proximal duodenum is seen, with no significant biliary duct dilatation.

immunodeficiency syndrome or those undergoing radiation therapy (14). The true incidence of duodenitis is unknown, given the difficulty of making a diagnosis without the use of endoscopy or imaging. Duodenitis manifests on cross-sectional images as thickening of the duodenal wall (Fig 19) (14,59). MR imaging shows duodenal wall thickening, with wide variability in the degree of enhancement on fat-saturated images (63).

Duodenal Crohn Disease.—Crohn disease may affect the duodenum, typically the first and second portions, and is associated with contiguous involvement of the stomach (59). The incidence of Crohn disease is 201 per 100,000, with the duodenum affected in 1%–2% of patients (64). Duodenal Crohn disease has imaging characteristics similar to those of Crohn disease located elsewhere in the small bowel, including thickened folds, ulcers, strictures, and fistula formation (Fig 20) (14,59,65). Rarely, duodenal Crohn disease may cause ampullary stenosis and biliary obstruction, with a prominent papilla seen at MRCP (66).

Duodenal Diverticula.—Duodenal diverticula commonly occur in the periampullary region because they are frequently found on the medial aspect of the descending portion of the duodenum (59). The incidence of juxtapapillary duodenal diverticula ranges from 0.16% to 23%, depending on the method of identification (radiography vs endoscopy) (67). At CT, the diverticula may be fluid filled, mimicking a pancreatic pseudocyst, or may contain foci of air, mimicking a pancreatic abscess (59). They may

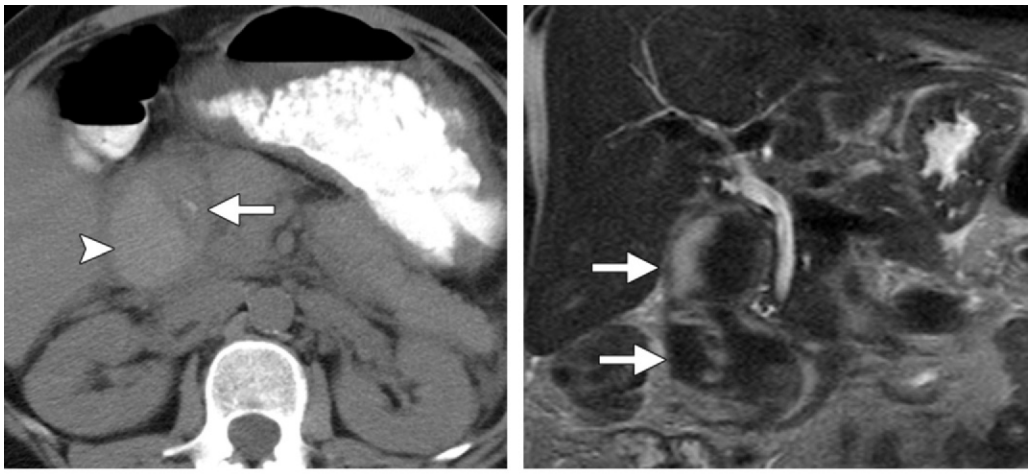

a. b.

Figure 21. Duodenal hematoma in a 37-year-old woman who was involved in an automobile collision. **(a)** Axial nonenhanced CT image shows a hyperattenuating hematoma (arrowhead) compressing the second portion of the duodenum (arrow). **(b)** Coronal T2-weighted HASTE MR image obtained 1 day after **a** because of elevated bilirubin levels shows mild dilatation of the CBD and intrahepatic duct due to extrinsic compression by the duodenal hematoma (arrows).

become impacted with intestinal debris, which leads to diverticulitis with signs of inflammation. At imaging, the identification of normal bowel gas or oral contrast material with direct communication to the adjacent duodenum aids in differentiating diverticula from other processes (12,15). Other complications include perforation, hemorrhage, and obstruction of the CBD or pancreatic duct (59).

Duodenal Perforation and Transection.— Duodenal perforation may occur secondary to a peptic ulcer or blunt or penetrating trauma. In 2006, 60,029 hospitalizations were attributed to duodenal peptic ulcers in the United States, with a 13.3% incidence of duodenal ulcer perforation (68). Duodenal perforation is a surgical emergency, but patients may not have impressive findings at physical examination because of the predominantly retroperitoneal location of the duodenum. CT is the primary imaging modality used to establish the diagnosis. Signs of duodenal perforation at CT include a periduodenal peritoneal fluid collection, duodenal wall edema, and fat stranding. Free retroperitoneal air may also be seen, with or without free intraperitoneal air (14,17).

Duodenal injuries result from compression trauma against the spinal column caused by deceleration injuries and seatbelt, handlebar, and sports injuries (69). They typically are subserosal and may be associated with duodenal narrowing. At CT, the most reliable sign of a duodenal hematoma is mixed attenuation, including areas of high attenuation from hemorrhage (69) (Fig 21). A duodenal hematoma must be differentiated from duodenal transection because transection is a surgical emergency and a hematoma is not.

Conclusion

The ampulla and periampullary region are difficult to assess radiologically, and the imaging characteristics of benign and malignant conditions in these areas overlap. Moreover, although some entities can be well evaluated with the high spatial resolution provided by CT, others are better assessed with the superior contrast resolution of MR imaging or MRCP. Knowledge of this region and its associated pathologic conditions is important to differentiate diseases that should be managed medically from those that require intervention.

References

1. Avisse C, Flament JB, Delattre JF. Ampulla of Vater: anatomic, embryologic, and surgical aspects. Surg Clin North Am 2000;80(1):201–212.
2. Kim JH, Kim MJ, Chung JJ, Lee WJ, Yoo HS, Lee JT. Differential diagnosis of periampullary carcinomas at MR imaging. RadioGraphics 2002;22(6):1335–1352.
3. Kim S, Lee NK, Lee JW, et al. CT evaluation of the bulging papilla with endoscopic correlation. RadioGraphics 2007;27(4):1023–1038.
4. Goodman MT, Yamamoto J. Descriptive study of gallbladder, extrahepatic bile duct, and ampullary cancers in the United States, 1997–2002. Cancer Causes Control 2007;18(4):415–422.
5. Jang KM, Kim SH, Lee SJ, Park HJ, Choi D, Hwang J. Added value of diffusion-weighted MR imaging in the diagnosis of ampullary carcinoma. Radiology 2013;266(2):491–501.

6. Chang S, Lim JH, Choi D, Kim SK, Lee WJ. Differentiation of ampullary tumor from benign papillary stricture by thin-section multidetector CT. Abdom Imaging 2008;33(4):457–462.
7. Kim TU, Kim S, Lee JW, et al. Ampulla of Vater: comprehensive anatomy, MR imaging of pathologic conditions, and correlation with endoscopy. Eur J Radiol 2008;66(1):48–64.
8. Wittekind C, Tannapfel A. Adenoma of the papilla and ampulla: premalignant lesions? Langenbecks Arch Surg 2001;386(3):172–175.
9. Sato T, Konishi K, Kimura H, et al. Adenoma and tiny carcinoma in adenoma of the papilla of Vater: p53 and PCNA. Hepatogastroenterology 1999;46 (27):1959–1962.
10. Lee M, Kim MJ, Park MS, Choi JY, Chung YE. Using multi-detector row CT to diagnose ampullary adenoma or adenocarcinoma in situ. Eur J Radiol 2011;80(3):e340–e345.
11. Carriaga MT, Henson DE. Liver, gallbladder, extrahepatic bile ducts, and pancreas. Cancer 1995;75 (suppl 1):S171–S190.
12. Yu J, Fulcher AS, Turner MA, Halvorsen RA. Normal anatomy and disease processes of the pancreatoduodenal groove: imaging features. AJR Am J Roentgenol 2004;183(3):839–846.
13. Vanderveen KA, Hussain HK. Magnetic resonance imaging of cholangiocarcinoma. Cancer Imaging 2004;4(2):104–115.
14. Jayaraman MV, Mayo-Smith WW, Movson JS, Dupuy DE, Wallach MT. CT of the duodenum: an overlooked segment gets its due. RadioGraphics 2001;21(Spec No):S147–S160.
15. Hernandez-Jover D, Pernas JC, Gonzalez-Ceballos S, Lupu I, Monill JM, Pérez C. Pancreatoduodenal junction: review of anatomy and pathologic conditions. J Gastrointest Surg 2011;15(7):1269–1281.
16. Bilimoria KY, Bentrem DJ, Wayne JD, Ko CY, Bennett CL, Talamonti MS. Small bowel cancer in the United States: changes in epidemiology, treatment, and survival over the last 20 years. Ann Surg 2009;249(1):63–71.
17. Pham DT, Hura SA, Willmann JK, Nino-Murcia M, Jeffrey RB Jr. Evaluation of periampullary pathology with CT volumetric oblique coronal reformations. AJR Am J Roentgenol 2009;193(3):W202–W208.
18. Tran T, Davila JA, El-Serag HB. The epidemiology of malignant gastrointestinal stromal tumors: an analysis of 1,458 cases from 1992 to 2000. Am J Gastroenterol 2005;100(1):162–168.
19. Neoptolemos J. Pancreatic cancer. New York, NY: Springer, 2010.
20. Chourmouzi D, Sinakos E, Papalavrentios L, Akriviadis E, Drevelegas A. Gastrointestinal stromal tumors: a pictorial review. J Gastrointestin Liver Dis 2009;18(3):379–383.
21. Sandrasegaran K, Rajesh A, Rushing DA, Rydberg J, Akisik FM, Henley JD. Gastrointestinal stromal tumors: CT and MRI findings. Eur Radiol 2005;15 (7):1407–1414.
22. Fang SH, Dong DJ, Chen FH, Jin M, Zhong BS. Small intestinal lipomas: diagnostic value of multislice CT enterography. World J Gastroenterol 2010; 16(21):2677–2681.
23. Siegel R, Naishadham D, Jemal A. Cancer statistics, 2012. CA Cancer J Clin 2012;62(1):10–29.
24. Miller FH, Rini NJ, Keppke AL. MRI of adenocarcinoma of the pancreas. AJR Am J Roentgenol 2006; 187(4):W365–W374.
25. Vachiranubhap B, Kim YH, Balci NC, Semelka RC. Magnetic resonance imaging of adenocarcinoma of the pancreas. Top Magn Reson Imaging 2009;20(1): 3–9.
26. Muniraj T, Vignesh S, Shetty S, Thiruvengadam S, Aslanian HR. Pancreatic neuroendocrine tumors. Dis Mon 2013;59(1):5–19.
27. Ro C, Chai W, Yu VE, Yu R. Pancreatic neuroendocrine tumors: biology, diagnosis,and treatment. Chin J Cancer 2013;32(6):312–324.
28. Bushnell DL, Baum RP. Standard imaging techniques for neuroendocrine tumors. Endocrinol Metab Clin North Am 2011;40(1):153–162, ix.
29. Bader TR, Semelka RC, Chiu VC, Armao DM, Woosley JT. MRI of carcinoid tumors: spectrum of appearances in the gastrointestinal tract and liver. J Magn Reson Imaging 2001;14(3):261–269.
30. Paulson EK, McDermott VG, Keogan MT, DeLong DM, Frederick MG, Nelson RC. Carcinoid metastases to the liver: role of triple-phase helical CT. Radiology 1998;206(1):143–150.
31. Kawamoto S, Johnson PT, Shi C, et al. Pancreatic neuroendocrine tumor with cystlike changes: evaluation with MDCT. AJR Am J Roentgenol 2013;200 (3):W283–W290.
32. Laffan TA, Horton KM, Klein AP, et al. Prevalence of unsuspected pancreatic cysts on MDCT. AJR Am J Roentgenol 2008;191(3):802–807.
33. Procacci C, Megibow AJ, Carbognin G, et al. Intraductal papillary mucinous tumor of the pancreas: a pictorial essay. RadioGraphics 1999;19(6): 1447–1463.
34. Drossman DA, Li Z, Andruzzi E, et al. U.S. householder survey of functional gastrointestinal disorders: prevalence, sociodemography, and health impact. Dig Dis Sci 1993;38(9):1569–1580.
35. Craanen ME, van Waesberghe JH, van der Peet DL, Loffeld RJ, Cuesta MA, Mulder CJ. Endoscopic ultrasound in patients with obstructive jaundice and inconclusive ultrasound and computer tomography findings. Eur J Gastroenterol Hepatol 2006;18(12): 1289–1292.
36. Tazuma S. Gallstone disease: epidemiology, pathogenesis, and classification of biliary stones (common bile duct and intrahepatic). Best Pract Res Clin Gastroenterol 2006;20(6):1075–1083.
37. Anderson SW, Rho E, Soto JA. Detection of biliary duct narrowing and choledocholithiasis: accuracy of portal venous phase multidetector CT. Radiology 2008;247(2):418–427.
38. Miller FH, Hwang CM, Gabriel H, Goodhartz LA, Omar AJ, Parsons WG 3rd. Contrast-enhanced helical CT of choledocholithiasis. AJR Am J Roentgenol 2003;181(1):125–130.
39. Romagnuolo J, Bardou M, Rahme E, Joseph L, Reinhold C, Barkun AN. Magnetic resonance cholangiopancreatography: a meta-analysis of test performance in suspected biliary disease. Ann Intern Med 2003;139(7):547–557.
40. Chalazonitis NA, Lachanis BS, Laspas F, Ptohis N, Tsimitselis G, Tzovara J. Pancreas divisum: magnetic resonance cholangiopancreatography findings. Singapore Med J 2008;49(11):951–954; quiz 955.
41. Soto JA, Lucey BC, Stuhlfaut JW. Pancreas divisum: depiction with multi-detector row CT. Radiology 2005;235(2):503–508.
42. DiMagno MJ, Wamsteker EJ. Pancreas divisum. Curr Gastroenterol Rep 2011;13(2):150–156.

43. Bernard JP, Sahel J, Giovannini M, Sarles H. Pancreas divisum is a probable cause of acute pancreatitis: a report of 137 cases. Pancreas 1990;5(3):248–254.
44. Byeon JS, Kim MH, Lee SK, et al. Santorinicele without pancreas divisum. Gastrointest Endosc 2003;58(5):800–803.
45. Nam KD, Joo KR, Jang JY, et al. A case of santorinicele without pancreas divisum: diagnosis with multi-detector row computed tomography. J Korean Med Sci 2006;21(2):358–360.
46. Akisik MF, Sandrasegaran K, Aisen AA, Maglinte DD, Sherman S, Lehman GA. Dynamic secretin-enhanced MR cholangiopancreatography. RadioGraphics 2006;26(3):665–677.
47. Barish MA, Yucel EK, Ferrucci JT. Magnetic resonance cholangiopancreatography. N Engl J Med 1999;341(4):258–264.
48. Ziegler KM, Pitt HA, Zyromski NJ, et al. Choledochoceles: are they choledochal cysts? Ann Surg 2010;252(4):683–690.
49. Park DH, Kim MH, Lee SK, et al. Can MRCP replace the diagnostic role of ERCP for patients with choledochal cysts? Gastrointest Endosc 2005;62(3):360–366.
50. Ladas SD, Katsogridakis I, Tassios P, Tastemiroglou T, Vrachliotis T, Raptis SA. Choledochocele, an overlooked diagnosis: report of 15 cases and review of 56 published reports from 1984 to 1992. Endoscopy 1995;27(3):233–239.
51. Manzelli A, Petrou A, Lazzaro A, Brennan N, Soonawalla Z, Friend P. Groove pancreatitis: a miniseries report and review of the literature. JOP 2011;12(3):230–233.
52. Triantopoulou C, Dervenis C, Giannakou N, Papailiou J, Prassopoulos P. Groove pancreatitis: a diagnostic challenge. Eur Radiol 2009;19(7):1736–1743.
53. Blasbalg R, Baroni RH, Costa DN, Machado MC. MRI features of groove pancreatitis. AJR Am J Roentgenol 2007;189(1):73–80.
54. Hart PA, Kamisawa T, Brugge WR, et al. Long-term outcomes of autoimmune pancreatitis: a multicentre, international analysis. Gut 2012; 62(12):1771-1776. http://gut.bmj.com/content/early/2012/12/10/gutjnl-2012-303617.full. Published December 11, 2012. Accessed December 20, 2012.
55. Krasinskas AM, Raina A, Khalid A, Tublin M, Yadav D. Autoimmune pancreatitis. Gastroenterol Clin North Am 2007;36(2):239–257, vii.
56. Sugumar A, Chari S. Autoimmune pancreatitis: an update. Expert Rev Gastroenterol Hepatol 2009;3(2):197–204.
57. Zen Y, Nakanuma Y. IgG4 cholangiopathy. Int J Hepatol 2012; 2012:article 472376. doi:10.1155/2012/472376. Published August 4, 2011. Accessed December 20, 2012.
58. Zhou LY, Xie XY, Chen D, Lü MD. Contrast-enhanced ultrasound in detection and follow-up of pancreaticoduodenal artery pseudoaneurysm: a case report. Chin Med J (Engl) 2011;124(17):2792–2794.
59. Brant WE, Helms CA. Fundamentals of diagnostic radiology. 3rd ed. Philadelphia, Pa: Lippincott, Williams & Wilkins, 2007.
60. Mayoral W, Salcedo JA, Montgomery E, Al-Kawas FH. Biliary obstruction and pancreatitis caused by Brunner's gland hyperplasia of the ampulla of Vater: a case report and review of the literature. Endoscopy 2000;32(12):998–1001.
61. Patel ND, Levy AD, Mehrotra AK, Sobin LH. Brunner's gland hyperplasia and hamartoma: imaging features with clinicopathologic correlation. AJR Am J Roentgenol 2006;187(3):715–722.
62. Hur S, Han JK, Kim MA, Bae JM, Choi BI. Brunner's gland hamartoma: computed tomographic findings with histopathologic correlation in 9 cases. J Comput Assist Tomogr 2010;34(4):543–547.
63. Marcos HB, Semelka RC, Noone TC, Woosley JT, Lee JK. MRI of normal and abnormal duodenum using half-fourier single-shot RARE and gadolinium-enhanced spoiled gradient echo sequences. Magn Reson Imaging 1999;17(6):869–880.
64. Nugent FW, Roy MA. Duodenal Crohn's disease: an analysis of 89 cases. Am J Gastroenterol 1989;84(3):249–254.
65. Poggioli G, Stocchi L, Laureti S, et al. Duodenal involvement of Crohn's disease: three different clinicopathologic patterns. Dis Colon Rectum 1997;40(2):179–183.
66. Yung K, Oviedo J, Farraye FA, Becker JM, Andrews CW Jr, Lichtenstein D. Ampullary stenosis with biliary obstruction in duodenal Crohn's disease: a case report and review of the literature. Dig Dis Sci 2005;50(6):1118–1121.
67. Zoepf T, Zoepf DS, Arnold JC, Benz C, Riemann JF. The relationship between juxtapapillary duodenal diverticula and disorders of the biliopancreatic system: analysis of 350 patients. Gastrointest Endosc 2001;54(1):56–61.
68. Wang YR, Richter JE, Dempsey DT. Trends and outcomes of hospitalizations for peptic ulcer disease in the United States, 1993 to 2006. Ann Surg 2010;251(1):51–58.
69. Linsenmaier U, Wirth S, Reiser M, Körner M. Diagnosis and classification of pancreatic and duodenal injuries in emergency radiology. RadioGraphics 2008;28(6):1591–1602.

Imaging Features of Benign and Malignant Ampullary and Periampullary Lesions

Paul Nikolaidis, MD • Nancy A. Hammond, MD • Kevin Day, MD • Vahid Yaghmai, MD • Cecil G. Wood III, MD • David S. Mosbach, MD • Carla B. Harmath, MD • Myles T. Taffel, MD • Jeanne M. Horowitz, MD • Senta M. Berggruen, MD • Frank H. Miller, MD

RadioGraphics 2014; 34:624–641 • **Published online** 10.1148/rg.343125191 • **Content Codes:** CT GI MR OI

Page 624
The term *ampulla* is defined as a dilated common channel that is formed where the two ducts combine. However, the use of this terminology is controversial because the presence of a common channel is inconstant, and actual dilatation of the common channel is unusual.

Page 625
The ampulla of Vater is surrounded by the sphincter of Oddi, a 1-cm structure composed of smooth muscle that regulates the flow of bile and pancreatic juices into the duodenum. The sphincter of Oddi surrounds a portion of the distal CBD, the distal main pancreatic duct, and the common channel (or, depending on the anatomy, the distal parallel channels).

Page 625
Ampullary cancer (adenocarcinoma) is a rare malignancy that arises from the distal biliary epithelium of the ampulla of Vater. Because of the central location of the lesion, patients often present with obstructive symptoms early in the disease process. Therefore, tumors may be discovered while they are still small and may be surgically resectable.

Page 633
Papillary stenosis is the blockage of bile or pancreatic fluid flow at the sphincter of Oddi in the absence of a mass or inflammatory lesion at the ampulla. It may manifest with pancreatitis, jaundice, or pain. The most common cause of papillary stenosis is sphincter of Oddi dysfunction, which can be either structural or functional.

Pages 634–635
In cases of suspected ampullary stenosis, secretin administration will cause persistent dilatation of the pancreatic duct. Increased pancreatic secretions caused by secretin administration will also distend the adjacent duodenum with fluid.